Proceedings World Geothermal Congress 2000
Kyushu - Tohoku, Japan, May 28 - June 10, 2000

DELINEATION OF A GEOTHERMAL RESERVOIR BY 2D INVERSION OF RESISTIVITY DATA AT HAMAM FARAUN AREA, SINAI, EGYPT.

Gad, El-Qady [1], Keisuke Ushijima[1] and El-Sayed.Ahmad. [2]

1-Geophys. Explor. Lab, Fac. of Eng., Kyushu University, 6-10-1 Hakozaki, Higashi-Ku, Fukuoka, Japan, 812-8581.
Ph.: +81-92-642-3643, Fax.: +81-92-642-3614, E-mail: gad@mine.kyushu-u.ac.jp
2- National Research Institute of Astronomy & Geophysics (NRIAG), Helwan, Cairo, Egypt.

Key words: geothermal, Resistivity, 2D inversion, Hamam Faraun, Sinai

ABSTRACT:
The Sinai Peninsula is one of the main geographic units of Egypt. Also, the Sinai Peninsula is considered to be an unstable shelf due to frequent earthquake activity and its relationship to the geologic setting of the area. Because of this, we directed the main aim of this work towards exploring the geothermal resources, and ground water aquifer at Hamam Faraun area, which is considered to be the hottest spring (72°C) in Sinai and in all of Egypt. A geoelectrical resistivity survey was conducted in terms of 17 VES using a Schlumberger array, of the maximum AB/2 =1000 m. Interpretation of a 1D inversion was performed to give a layered resistivity earth using a non-linear least squares method. However, some resistivity sections of the 1D inversion are not fully understood because of the complicated geological structure. Therefore, we have carried out a 2D inversion based on ABIC least squares method for the same data set. The general distribution of resistivity shows a very low value near the Hamam Faraun hot spring. However, the cross section derived from the 2D inversion still shows a rough spatial resistivity distribution which corresponds to the abrupt changes of resistivity distribution between two neighboring blocks. It clearly elaborates the subsurface structure at Hamam Faraun area as well as elucidates and gives an explanation for the hot water source in the area. It is concluded that the hydrothermal system at Hamam Faraun area is derived from 1D and 2D inversion results of vertical electric sounding data with Schlumberger electrode array. However, other geoelectrical methods such as MT or EM are recommended to overcome seawater intrusion and topography problems.

1.INTRODUCTION:

The Sinai Peninsula lies at the crossroads of the continents of Africa and Asia, and actually represents the Asiatic part of Egypt. Above all, the beauty of scenery, the cradle of heavenly religions (Judaism, Christianity and Islam). It has always been evident that the Sinai region has great economic development potential. However such development depends critically on peace and stability in the region, which has not been a reality until recent times. Also as this part is considered to be an unstable shelf due to the frequent earthquake activity and its relation with geologic setting of the area, which is controlled by the structure activity of the Red sea, Gulfs of Suez and Aqaba. Now, Sinai is moving rapidly towards huge investments in development. Because of this, the main aim of this work has been directed towards exploring some of natural resources in that area. Among these resources are both of geothermal resources, as one of clean energy resources, and ground water aquifer. Since the Hamam Faraun area as shown in Fig. (1) has surface geothermal manifestations and is considered to be the hottest spring (72°C) in Sinai and in all of Egypt, it is the most suitable area for conducting this investigation.

DC resistivity has been used with great success for locating geothermal aquifers (Arnason et, al., 1987 and Cheng, 1980) especially in a resistive environment, as is the case in many low temperature fields (Flovenz and Georgsson, 1982). However, it has been unsuccessful in outlining the reservoir of vapor-dominated systems located in sedimentary rocks (Alfano, 1961 and Hochstein, 1975).With the increased availability of faster computers, it is now practical to employ numerical modeling techniques to invert resistivity data for an actual geologic structure. However, there has been little success in overcoming the uniqueness problem associated with uncertain and incomplete geophysical data. In this study, we have carried out a 2D inversion based on the ABIC least squares method for a Schlumberger VES data set measured at H. Faraun area.

The geological environment of geothermal fields differs substantially from one field to another. Factors such as topography, surface rock conditions, type of host rock, tectonic regime, heat source and fluid type are variables controlling the geophysical characteristics of the geothermal field.

2.TOPOGRAPHY AND GEOLOGICAL SETTING:

The geology of Sinai Peninsula is more complicated and represented for all geologic time. The Hamam Faraun area is of more vigorous topography because of the presence of several local mountain areas (G. H. Faraun, and G. Tall) of altitudes varying from 50 to 480 m above sea level. The shallow geological succession in the study area is distinguished into sand, conglomerate, sandy limestone, lagoonal gypsum, limestone, shall, limestone and chalk with flinty limestone. This varies in age from Post Pliocene, Pliocene, Miocene, Oligocene, Eocene and upper cretaceous respectively (Said 1962).

In the early Tertiary period (Oligo - Miocene), with the opening of the Red Sea rift, some volcanic activity took place. In western and central Sinai, a number of basaltic bodies mostly of doleritic dikes, sills, plugs and flows are known to exist near Abu Zenima and H.Faraun (Meneisy, 1990). The major geological structural feature of the study area is a well defined fault block oriented NNW-SSE, which tilts strongly eastward on its western side. Also there is a fault escarpment overlooking directly to the Gulf of Suez and rising about 300 m above the Gulf (El-Shinnawi and Sultan, 1973).

3.GEOTHERMAL REGIME:

The Hamam Faraun area is characterized by several hot springs lying at the foot of Gebel H. Faraun along a more or less straight line extending about one km along the Gulf of Suez coast. The fault forms a steep cliff bordering the Gulf of Suez. Two groups of thermal springs were found. The northern group (72 °C) issues on land while the southern group emerges beneath the surface of the Gulf's water. The cliff above the spring is composed of dolomite. The heat source for these springs is probably derived from high heat flow and deep circulation controlled by faults associated with the opening of the Red Sea and Gulf of Suez rifts. It is supposed that the spring's water is presumably a mixture of brine and water of Pleistocene contained in the Nubian sandstone aquifer which infiltrated the outcrops on the highland of Sinai and emerged along the fault lines bordering Sinai peninsula (Magaritz and Issar, 1973).

4.GEOPHYSICAL EXPLORATION:

The geophysical survey described in this work has been carried out by DC resistivity sounding with Schlumberger array. A 17 VES stations were measured as shown in Fig. (1), using electrode spacing started from AB/2= 2 up to 1000 m, in a successive steps. The field sites were chosen on the basis of the accessibility and applicability of the Schlumberger method.

A 1D interpretation using the least squares method had been conducted (El-Qady, et al., 1998). A general outlook to the interpretation of the VESes' curves reveals that the number of the interpreted layers varies from five to seven layers through the study area. The true resistivities of these layers vary from 0.2 to 60819 ohm-m, while the thickness varies from 0.9 to 291 m. Although the deduced information from 1D cross section was correlated with the geological studies and surface thermal manifestations, it is not fully understood for 3D geological structure. To get an understandable solution we have to use 2D or 3D inversion. In this work we present a 2D inversion for the same data set using Uchida's (1991) algorithm. This algorithm is based on the ABIC (Akaike Bayesian Information Criterion, Akaike, 1980) algorithm to obtain convergence to a solution with the optimum smoothness using a Finite Element calculation mesh.

4.1.Theoretical Basis:

This 2D algorithm considers a 2D-earth model whose resistivity varies along the X-and Z- axis and doesn't change along Y-axis. Since the current is injected at a point on the surface, however it flows three dimensionally in the earth. The response in a 2D earth is given by Poisson's equation as:

$$- \nabla [\sigma(x,z)\nabla V(x,y,z)] = I(x,y,z), \qquad (1)$$

where $\sigma(x, z)$ is the conductivity, v (x, y, z) is the electric potential and I(x,y,z) represents the source current intensity. By applying the Fourier transform to equation (1) with respect to the y coordinate, we obtain:

$$-\nabla. [\sigma(x,z)\nabla \hat{V}(x,k_y,z)] + k_y^2 \sigma(x,z)\hat{V}(x,k_y,z) = \hat{I}(x,k_y,z), \qquad (2)$$

where ^ means the Fourier transform and k_y is the Fourier transform variable. A detailed explanation of the finite element discretization of equation (2) is given in Sasaki (1981). Discretization over mesh yields a matrix equation,

$$KV = S, \qquad (3)$$

where K is an L x L spare band matrix with positive symmetric values. This is determined by the geometry and conductivity of each finite element, L is the number of nodes, V is a column vector of the unknown potential at each node, and S is the column vector of current source intensity at each node. The potential V in real 3D domain can be obtained by solving Eq. 3 and applying inverse Fourier transform,

$$\Delta V(x,0,z) = (1/\pi)\int_0^\infty \hat{V}(x,k_y,z)dk_y, \qquad (4)$$

and the apparent resistivity for Schlumberger can be calculated as:

$$\rho_a = \frac{G\Delta V}{I}, \qquad (5)$$

where G is the geometrical factor, and ΔV is the calculated potential difference between the receiving electrodes, M and N. Here it describes the 2D model, which holds its block boundaries during the inversion and only the resistivity within each block changes with the iteration procedure. The misfit (ϕ) of the data is determined by the following equation:

$$\phi = \frac{1}{N}\sum_{j=1}^{N}\{y_j^o - y_j^c(x)\}^2, \qquad (6)$$

where (y_j^o) is the observed data and (y_j^c) is the calculated data. If we consider the (k-1) - th iteration of the inversion process. Applying a Taylor expansion to $y_j(x)$ at $x^{(k-1)}$ and neglecting the terms of the second and higher order we obtain:

$$y_j(x^{(k)}) = y_j(x^{(k-1)}) + \sum_{i=1}^{M}\left(\frac{\partial y_j}{\partial x_i}\right)_{x^{(k-1)}} \Delta x_i^k, \qquad (7)$$

where (k) means k-th iteration. In order to minimize the misfit ϕ, the condition $\frac{\partial \phi}{\partial x_i} = 0$ shall be satisfied, Uchida, (1991).

A statistical criterion, ABIC (Akaike Bayesian Information Criterion) has been proposed by Akaike (1980), by applying the maximum entropy theorem to the Bayesian statistics. ABIC is derived to provide an index for finding the maximum Bayesian likelihood as:

$$ABIC = 2\log(\max.L(m/d)) + 2\dim(\text{hyperparameter}), \qquad (8)$$

where L (m/d) is the Bayesian likelihood and the hyperparameter means a parameter, which is not used to express the model directly, but used to obtain parameters of the model. The only hyperparameter in this case is the smoothing parameter (α). Further explanation of the equations was described by (Uchida, 1993), then ABIC can be written as:

$$ABIC(\alpha) = N\log(2\pi\frac{U}{N}) \quad -\log\left|\alpha^2 C^T C\right|$$
$$+\log\left|(WA)^T(WA)\right| + \alpha^2 C^T C + N + 2\,, \qquad (9)$$

where, d is a set of observed data, A is a Jacobian matrix defined by $A_{ij}=\partial y_i/\partial \rho_j$, m, is a hypothetical model, W, is a diagonal weighting C, is a roughness matrix of a model parameter, which gives the finite difference of the model parameters between laterally and vertically adjacent blocks and U is a function defined as:

U=misfit + roughness penality of the model

$$= \phi + \alpha^2\|Cm\|^2\,, \qquad (10)$$

4.2. Inversion Results:

For the least-square inversion with smoothness regularization, we seek a model that minimizes both the data misfit and model roughness. From a statistical point of view, ABIC works as an index to determine the maximum likelihood of the model. That means that a smaller ABIC indicates a larger likelihood and higher entropy, hence give a best fit model. This also means the optimum smoothness is judged by minimizing ABIC, which makes the convergence and the selection of the optimum smoothness the objective. So, we have to run the inversion process until the best fit is attained.

The program outputs 7 models per iteration with different 7 values for the inversion parameters. Then it selects the best model according to the smoothing factor and rms misfit as an initial model for the next iteration. Figure 2 shows the rms misfit and the smoothing factor (α) as a function of iteration number. As it is obvious in figure 2, (a), for the profile A-A', the rms attains minima after the second iteration, smoothing factor (α) attains it at the fifth iteration. For the profile (D-D') (α) attains minima at the seventh iteration figure 2, (b), as well as it attains it at the third iteration for the profile (E-E') figure 2, (c).

Since we have 7 models per iteration, we should investigate the behavior of the inversion parameters per iteration, as shown in Figure (3) for the profile (A-A'). In the first iteration, the parameters curve gives a higher amplitude and wide range of variation, which mean a rough model. As the iteration processes proceeds, ABIC, figure3, (a) becomes smaller and no visible change at the fifth iteration. Figure 3, (b) shows a nearly straight line for fitting values at the fifth iteration as well as in figure 3, (c and d) for the smoothing factor and roughness, respectively. This indicates that the fifth iteration's model is the best-fit model for this profile (A-A'). The same analysis and inspection have been studied for the other four profiles, which informed us that the best fit model is attained after the fifth, third, seventh and fourth iterations for the profiles B-B', C-C', D-D' and E-E' respectively.

4.3. 2D Cross-Section:

According to the results obtained through the inversion process, we should be able to construct the 2D-geoelectrical cross section for each profile. This depends on which iteration minimizes ABIC and gets the convergence. Figure (4) shows the 2D cross section of the inverted model after the fifth iteration for the profile (A-A'). The initial model is assumed to be a 100 Ohm.m homogeneous earth and the topography is incorporated into the model. The number of the observed data used for the inversion is 100 while the number of resistivity blocks is 84. The general feature of this inverted section is a huge thick low resistive body in the northern part of the profile (VESes, 17,1 and 2). This correlated with the Gypsum deposits in that area. Meanwhile may reflect the Seawater intrusion. In the southern part, around the hot spring, the basement uplift is elaborated. This may give a suggestion and explanation for the origin of the hot water at H. Faraun hot spring.

The integrated 2D-geoelectrical cross-section for the H. Faraun area, figure (5), provides valuable information that enables configuration of the subsurface structure at the study area. It is also elucidated that:

- There are two main structure-faulting systems in NNW-SSE and E-W directions affecting the area.
- There is a quite thick (~100m) aquifer around H. Faraun hot spring, which is considered as a promising area for geothermal drilling.

5. CONCLUSION:

The present work aimed to delineate and elucidate the geothermal reservoir at H. Faraun hot spring using ABIC least square 2D inversion of Schlumberger resistivity sounding measured at the area. According to the results obtained, we conclude that the inversion procedure can reduce the misfit through the iteration. The 2D resultant cross section had been correlated with 1D inversion. However, the 2D cross section elaborates the geological structure at the study area, which is correlated with the previous geological studies.
According to the 2D interpretation of these data set a promising area for geothermal drilling is highly recommended, especially around the hot spring, and its neighboring areas (VESes, 2 and 3), where there is an arial extent and quite considerable aquifer thickness reaches more than 100 m.

2D cross section elucidates and gives explanation to the origin of the hot water source at the study area.

6. RECOMMENDATION:

Detailed geophysical survey is recommend using different geophysical resistivity tools like Magnetotelluric and Electromagnetic methods, which can overcome the problem of topography and sea water intrusion in this area. However, using different techniques of 2-D or 3-D in the interpretation is recommended more strongly.

7. ACKNOWLEDGEMENT:

The authors would like to express their deepest and sincere thanks to the National Research Institute of Astronomy and Geophysics (NRIAG), Egypt, for a constructive guidance and kind official facilities required for data acquisition in this work. Sincere thanks to all the staff of Exploration Geophysics Lab in Kyushu University for their continuous guidance and support during this work. Moreover, the authors are thankful to the anonymous reviewers for their constructive criticism, which helped to improve the manuscript to its present form.

8. REFERENCES:

Akaike, H., (1980). Likelihood and Bayes procedure, In: Bayesian statistics, J.M. Bernardo, et. al.(Ed)., Univ. press, Valencia, Spain.PP.143-166.

Alfano, L., (1961). Geoelectrical explorations for natural steam near ''Monte Amiata'': Quad. Geofisica Appl., V.21 P.3

Arnason, K., Flovenz, O., Georgsson, L. and Hersir, G., (1987). Resistivity structure of high temperature geothermal systems in Iceland. IUGG, XIX General assembly, Vancouver, V. 2: 477.

Cheng, Y., (1980). Location of near surface faults in geothermal prospecting by the combined Head-on resistivity profiling method. Proc. New Zealand Geothermal Workshop, 163-166.

El-Shinnawi M.A and Sultan, I., (1973). Lithostratigraphy of some subsurface upper cretaceous sections in the Gulf of Suez area, Egypt, Actas Geol. Hungaria, Vol., 17, 469-493.

EL-Qady, G.; Hassaneen, A., Gh.; and Ushijima, K., (1998). Reconnaissance electrical Resistivity survey of geothermal reservoir at H. Faraun hot spring, Sinai, Egypt. Proc. of the 99th SEGJ, Oct. 20-23, 1998, Tokyo, Japan.

Flovenz, O. and Georgsson, L., (1982). Prospecting for near vertical aquifers in low temperature geothermal areas in Iceland, Trans.Geotherm.Resour. Counc. 6, 19-22.

Hochstein, M.P., (1975). Geophysical exploration of the Kawah Kamojang field, West Java. 2nd UN symposium on the exploration and development of geothermal resources, Vol.2 Pp.1049-1058.

Magaritz, M. and Issar, A., (1973). Carbon and Oxygen isotopes in epigenetic hydrothermal rocks from H. El-Farun, Sinai. Chemical Geology, 12, 137-146.

Meneisy, M.Y., (1990). Volcanicity, Chapt.9, In Said, R.(Ed.) 1990. Geology of Egypt, Balkema Pub. Rotterdam, Netherlands, 157-172.

Said, R., (1962). The geology of Egypt. Elsevier, Amsterdam-New York, pp.1-377.

Sasaki, Y.,(1981). Automatic interpretation of resistivity sounding data over two-dimensional structures (I) (in Japanese), Geophys. Explor. of Japan (Butsuri Tanko), 34, 341-350.

Uchida, T., (1991). 2D resistivity inversion for Schlumberger sounding. Butsuri -Tansa Vol.44 No.1, .1-17.

Uchida, T.(1993). Smooth 2-D inversion for Magnetotelluric Data Based on Statistical Criterion ABIC. J.Geomag. Geoelectr., 45,841-858.

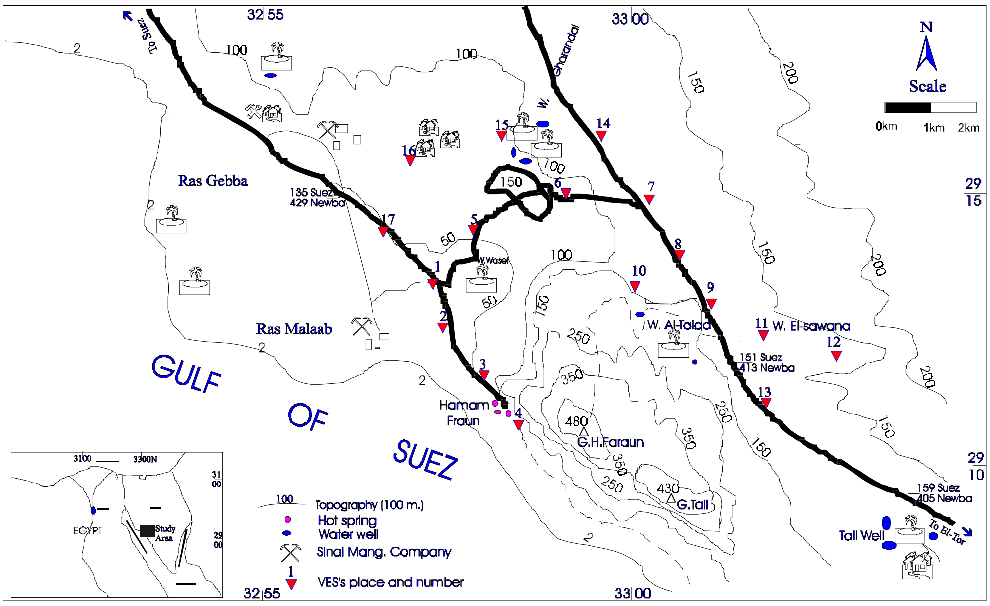

Fig.1. Location map for the geophysical survey at Hamam Fraun Area.

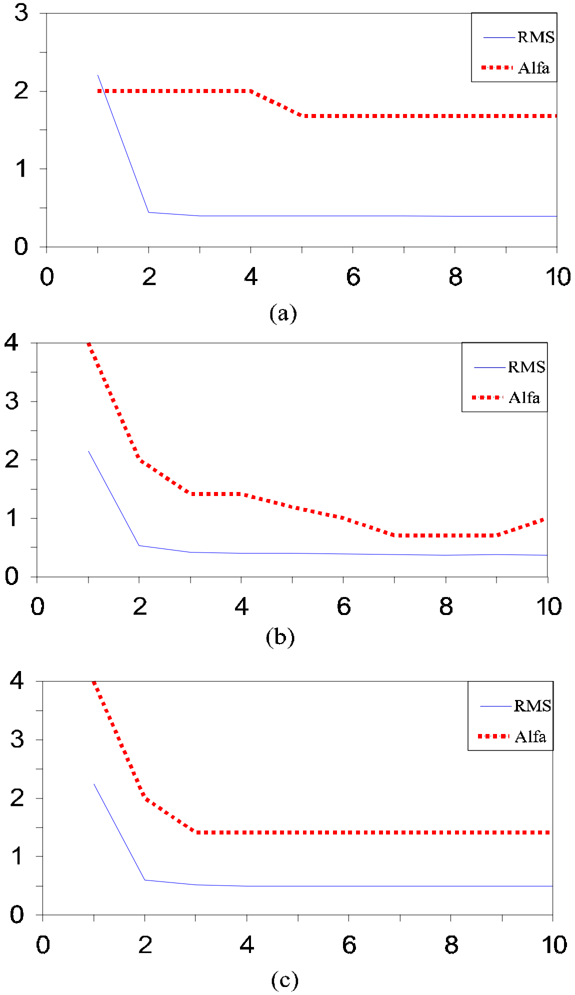

Figure 2. The rms misfit and alfa as
a function of the iteration numbers
(a) the profile (A-A'), (b)the profile (D-D'),
and (c) the profile (E-E').

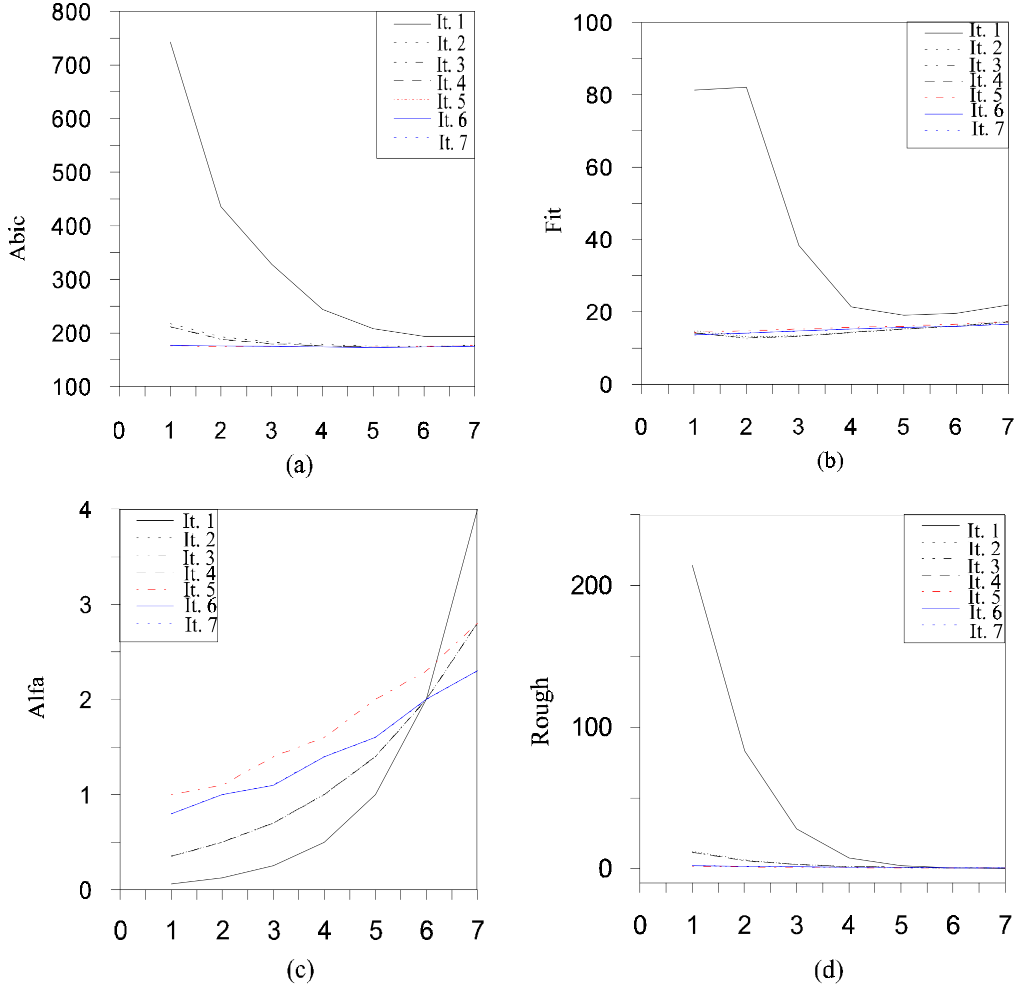

Figure 3. The inversion parameters as a function of the iteration
numbers for the profile (A-A'), (a) ABIC, (b) rms misfit,
(c) smoothing factor, and (d) Roughness.

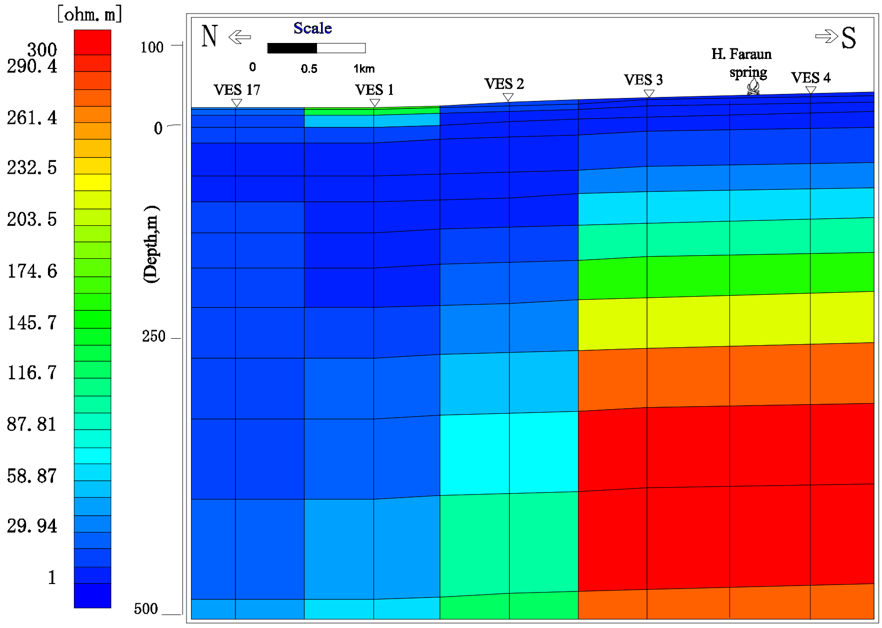

Figure 4. Inverted Geoelectrical Cross Section of the Profile A-A'.

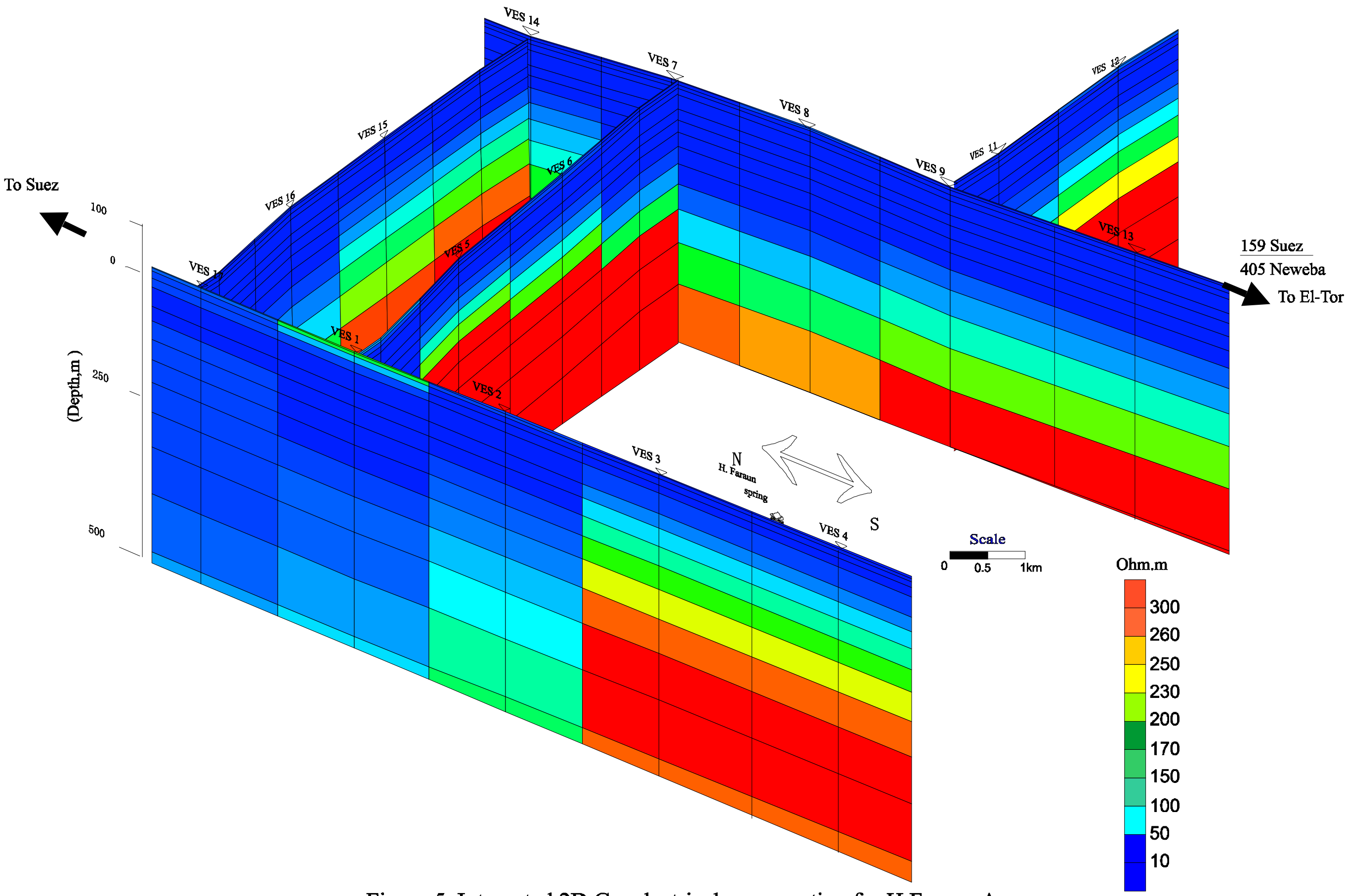

Figure 5. Integrated 2D Geoelectrical cross section for H.Faraun Area.